AIP | Review of Scientific Instruments

Biaxial stress ring applications to magneto-optical studies of semiconductor films

Marcio Peron Franco de Godoy, Marcelo K. K. Nakaema, Fernando Iikawa, Wilson Carvalho Jr., Evaldo Ribeiro, and Angelo L. Gobbi

Citation: Review of Scientific Instruments **75**, 1947 (2004); doi: 10.1063/1.1753090
View online: http://dx.doi.org/10.1063/1.1753090
View Table of Contents: http://scitation.aip.org/content/aip/journal/rsi/75/6?ver=pdfcov
Published by the AIP Publishing

Biaxial stress ring applications to magneto-optical studies of semiconductor films

Marcio Peron Franco de Godoy,[a] Marcelo K. K. Nakaema, and Fernando Iikawa
Instituto de Física "Gleb Wataghin," UNICAMP, Campinas-SP, C.P. 6165, 13083-970, Brazil

Wilson Carvalho, Jr., Evaldo Ribeiro, and Angelo L. Gobbi
Laboratório Nacional de Luz Síncrotron, CP-6192, 13084-971 Campinas-SP, Brazil

(Received 29 September 2003; accepted 20 February 2004; published online 21 May 2004)

We present a magneto-optical system to study semiconductor heterostructures in the presence of an external biaxial tensile strain. The pressure cell is based on the deflection of a plate (the sample) placed between a sphere and a ring. This externally applied stress is easily controlled and can achieve a deformation of up to ~0.25% for GaAs films. This device is very useful for band structure study and optical resonance experiments in heterostructures. We also present the application of the device to study the behavior of the magneto-excitons in InP epitaxial layer as a function of the biaxial strain. We observed that the diamagnetic and Zeeman effects in InP films are affected by the biaxial tensile strain. © *2004 American Institute of Physics.* [DOI: 10.1063/1.1753090]

I. INTRODUCTION

In the last decades, semiconductor films such as heterostructures have been studied under external pressure by optical and magneto-transport measurements using hydrostatic[1–3] and uniaxial pressure systems,[4,5] and recently biaxial ones.[6–8] The application of an external pressure is a powerful method for investigating the physical properties of strained-layer heterostructures grown by epitaxial techniques. These layers are obtained by growing a thin layer of a given material on a lattice mismatched substrate, so that the epitaxial layer is under a built-in biaxial strain. The strain directly affects the electronic structure of the material and, as a consequence, their optical and transport properties are altered. This means that the strain can be used as a controllable parameter for performing a heterostructure band gap engineering.[6] An important point relative to the optical properties is that the valence band mixing induced by strain strongly contributes to the spin relaxation of holes[9] in semiconductor heterostructures. Moreover, the g factor is also altered by the valence band mixing. Information on these parameters is essential for spin-related problems relative to the promising new fields of spintronics.

In this work, we present a special pressure cell that can be used in a magneto-cryostat to study magneto-optical and -transport properties. The pressure cell is based on the bending of a plate placed between a ring and a sphere, a principle which is similar to those reported in the literature.[10,11] Our system, to the best of our knowledge, is unique since it was designed to work at low temperatures in the presence of a magnetic field, allowing magneto-optical and magneto-transport measurements in semiconductor heterostructures as a function of an externally applied biaxial strain. We present results of an application of the system for investigating both the diamagnetic shift and the Zeeman splitting in semiconductors.

II. THEORY

A. The bending plate model

We model the deformation of the plate using the theory of elasticity,[12] where the strain is a tensor with elements ϵ_{ij} given by the differential of the elongations u, v, and w along the x, y, and z axes, respectively, in Cartesian coordinates:

$$\epsilon_{xx}=\frac{\partial u}{\partial x}, \quad \epsilon_{xy}=\frac{\partial v}{\partial x}+\frac{\partial u}{\partial y},$$
$$\epsilon_{yy}=\frac{\partial v}{\partial y}, \quad \epsilon_{yz}=\frac{\partial w}{\partial y}+\frac{\partial v}{\partial z}, \tag{1}$$
$$\epsilon_{zz}=\frac{\partial w}{\partial z}, \quad \epsilon_{zx}=\frac{\partial u}{\partial z}+\frac{\partial w}{\partial x}.$$

We consider here the sample as a circular plate (a disc), with thickness h much smaller than the other dimensions, placed between a ring, with a radius R, and a sphere with a radius close to R, see Fig. 1(a). The deflection w is assumed to be much smaller than h. For a small deformation the plane that cuts the plate at the middle [$z=0$, dashed line in Fig. 1(a)] is free of deformations. The upper side of the plate is under a tensile strain, while the lower side is under compression. The deflection w caused by a load $q(x,y)$ placed at the center of the plate can be obtained by solving[12]

$$\nabla^2\nabla^2 w=\frac{q(x,y)}{D}, \tag{2}$$

where D is the rigidity coefficient. Due to the deflection symmetry, it is advantageous to transform our equations to cylindrical coordinates (r,ϕ,z) instead of the (x,y,z) coordinates. The boundary conditions are such that the force moment and deflection at the edge are null:

[a]Electronic mail: mgodoy@ifi.unicamp.br

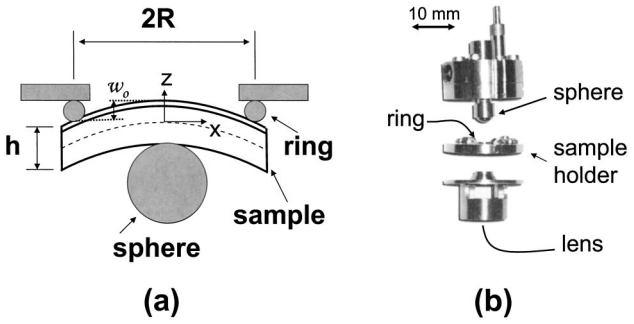

FIG. 1. (a) Schematic diagram of the sample placed between a sphere and a ring. (b) Lateral view of the biaxial pressure cell divided in three parts: sphere, sample holder (ring) and lens.

$$\left(\frac{\partial^2}{\partial r^2}+\frac{\sigma}{r}\frac{\partial}{\partial r}\right)w(R)=0 \tag{3}$$

and

$$w(R)=0, \tag{4}$$

where σ is the Poisson ratio. As a first approximation, the solution of Eq. (2) is

$$w(r)=\frac{w_0(1+\sigma)}{R^4(5+\sigma)}\left\{(R^2-r^2)^2+4R^2\frac{(R^2-r^2)}{(1+\sigma)}\right\}, \tag{5}$$

where

$$w_0=w(0)=\frac{qr^4}{64D}\left\{\frac{(5+\sigma)}{(1+\sigma)}\right\} \tag{6}$$

is the deflection at $r=0$. For crystals with zinc-blende symmetry, such as InP, GaAs and their alloy compounds, $D=h^3C_{11}/12$ and $\sigma=C_{12}/C_{11}$, where C_{ij} are the elements of the elastic constant tensor of the material. At the center of the disc the strain is symmetric and for crystal orientation such that the biaxial strain is in the (001) plane: $\epsilon_{xx}=\epsilon_{yy}=\epsilon$. We use here $\epsilon>0$ when the lattice parameter increases, i.e., a tensile strain, and $\epsilon<0$ for the compressive strain. Using the Hooke's law, we find the strain

$$\epsilon=\frac{4(1+\sigma)(3+\sigma)}{R^2(1-\sigma)(1+2\sigma)(5+\sigma)}w_0z. \tag{7}$$

Usually, semiconductor heterostructures consist of a thickness varying from 5 to 500 monolayers of a single or a sequence of different material layers and thicknesses grown on a thick substrate at ~0.5 mm. Therefore we are usually interested in applying biaxial strain near the sample surface. According to Fig. 1(a), $z=+h/2$ corresponds to the strain at the surface of the disk. The strain depends linearly on the deflection w_0 of the plate at the center $r=0$. We can also estimate the force applied by the sphere on the disk:

$$F=\frac{16\pi C_{11}}{3R^2}\frac{(1+\sigma)}{(5+\sigma)}w_0h^3. \tag{8}$$

Our apparatus was designed to apply forces as large as 200 N; for sample thickness of 0.5 mm and a sphere radius $R=4$ mm. These parameters allow us to produce deflections of order 50 μm in GaAs.

B. Energy bands of a semiconductor under biaxial strain

The crystal treated here has a zinc-blende symmetry and a direct gap band structure, where the top of the valence band (VB) and the bottom of the conduction band (CB) are both at the center (Γ point) of the Brillouin zone ($k=0$). The top of the VB is degenerate formed by the heavy hole (HH) and the light hole (LH) bands. The influence of the strain on the band structure is well known. In the case of the crystal under biaxial strain along the (001) plane, where it breaks the cubic symmetry, the gap energy is governed by the solutions for the Bir-Pikus Hamiltonian and at $k=0$ they become[13]

$$\begin{aligned}E_g^{\mathrm{HH}}&=E_g^0+\delta E_c-\delta E_{v2},\\ E_g^{\mathrm{LH}}&=E_g^0+\delta E_c-\delta E_{v1},\end{aligned} \tag{9}$$

where

$$\begin{aligned}\delta E_c&=2a(1-\sigma)\epsilon,\\ \delta E_{v1}&=-b(1+2\sigma)\epsilon+2\frac{b^2(1+2\sigma)^2\epsilon^2}{\Delta_0},\\ \delta E_{v2}&=b(1+2\sigma)\epsilon.\end{aligned} \tag{10}$$

E_g^{HH} and E_g^{LH} are the energy separation between the bottom of the CB and the top of the HH and LH bands at $k=0$, respectively, a is the hydrostatic deformation potential, b is the shear deformation potential for tetragonal symmetry, δE_c is the conduction band displacement due to hydrostatic component, and Δ_0 is the spin–orbit splitting energy.

For a bulk material the energy gap of the semiconductor increases for $\epsilon<0$ (compressive) and the top of the VB becomes the HH band; whereas the energy gap decreases for $\epsilon>0$ and the top of the VB becomes the LH band. In our experimental configuration the epitaxial film is under a tensile strain; in this case, the lower energy transition measured by photoluminescence technique is due to light-hole excitons. The strain ϵ is extracted by evaluating the strain dependent gap energy [Eq. (9)] using the material parameters and the experimental transition energy.

III. DESCRIPTION OF THE PRESSURE CELL

The pressure cell is divided in three mechanical parts [see Fig. 1(b)]. The first one is comprised of the sphere and of a set of gears externally controlled in order to move the sphere toward the sample. The second part contains the sample holder and the ring, with a radius of 4 mm. The sample is fixed using a soft metal clamp. The third part is related to the optical measurements; it contains a lens that is used both to focus the laser beam and to collect the luminescence. The sample size used here is 10×10 mm^2. The sphere is moved to push the sample against the ring [see Fig. 1(b)]. At the center of the ring, which is at the opposite side of the sphere, the sample surface, where the epitaxial film lies, is under symmetric and maximum biaxial tensile strain. Since in the photoluminescence experiments only the region under the laser spot is probed, we can select the region where the strain is maximum. The dimensions and material of the pressure cell were designed to fit on an optical magneto-cryostat

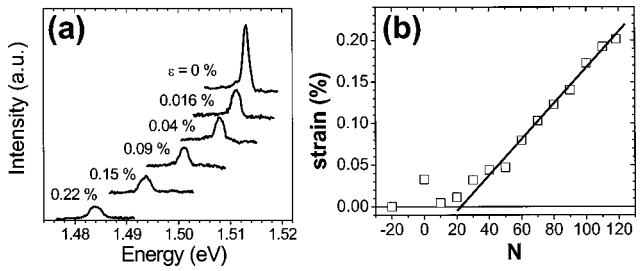

FIG. 2. (a) Typical 2 K PL spectra of a thick GaAs film for different biaxial strain. (b) Plot of the strain as a function of the number of turns N.

(Oxford Instruments) used for temperatures ranging from 1.8 to 300 K and magnetic field up to 17 T. The sphere motion is externally controlled by a step-motor. Each turn of the motor axle corresponds to a sphere displacement of approximately 0.5 μm corresponding to the sample deflection w_0. The precision of centering and the mechanical stability of the sphere relative to the ring are crucial to obtain the highest possible strain on the film without breaking the sample. The surface of the ring and the sphere must also be polished. We do not use any grease in the gears because the cell is meant to operate at very low temperatures. We also used the same material (nonmagnetic stainless steel) for all mechanical parts in order to avoid differences of the thermal expansion coefficients.

IV. EXPERIMENTAL RESULTS AND DISCUSSIONS

We used two samples, 300 nm of InP and GaAs epitaxial films grown by metalorganic chemical vapor deposition on a 360 μm InP (001) and GaAs (001) undoped substrate, respectively. On the back of the sample we deposited a thin metal film used for electric contact to indicate when the sphere touches the sample, i.e., when it starts to apply the stress on the sample. The backlash of the gears in this cell is $\sim$20 μm. The photoluminescence (PL) and magneto-photoluminescence (magneto-PL) experiments were performed using a He–Ne laser for excitation and a triple monochromator with CCD detector. For the measurements under magnetic fields, we used a quarter-wave plate and a linear polarizer to choose the circularly polarized luminescence, in order to select the two optical active exciton components. In the following we present the test of the pressure cell using GaAs epitaxial film and the results of the magneto-exciton emission in InP films in the presence of biaxial strain.

A. Test and calibration of the pressure cell using GaAs films

Since the optical and electronic constants of bulk GaAs are well known,[14] this is an appropriate system to test the pressure cell. Figure 2 shows the PL spectra of the GaAs sample for different tensile strains. The optical emissions are attributed to the bound bulk exciton recombination for the unstrained case and the bound light hole exciton for strained cases. The bound excitons are associated to the residual shallow impurities of the sample. We also plot the energy shift of the PL peak as a function of the number of turns N of the step-motor, $N=0$ corresponds to the point where the sphere just touches the back of the sample. The PL intensity of the

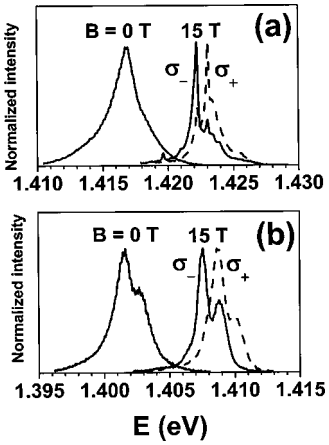

FIG. 3. Magneto-PL spectra of InP film for 0 and 15 T: (a) for $\epsilon=0$ and (b) for $\epsilon=0.15\%$. σ_+ and σ_- represent the right and left circular polarization of the luminescence.

spectra shown in Fig. 2 diminishes for applied strain because the oscillator strength of the light-hole is smaller than that of the heavy-hole transitions (bulk exciton).[15] We used Eq. (9) (and the bulk parameters from Ref. 14) for the LH transition in order to determine the corresponding strain from the PL peak energy shift. During the first turns we observe oscillations of the PL peak energy, which are due to the accommodation of the whole mechanical system (the sample and the pressure cell). We observe that the sample has effectively a linear behavior of the strain with the shift of the sphere only after $N=20$ turns, as shown in Fig. 2(b). For N above 20 we estimate the sphere displacement per turn from the slope of the straight line and Eq. (7) obtaining 0.54 ($\pm$0.05) μm, which is in a good agreement with the value estimated for our pressure cell, which is 0.5 μm per turn. This result also indicates that our theoretical model describes well the bending of the sample.

We note that the linewidth of the PL peak increases when the sample is strained. This broadening is attributed to the gradient of the strain along the z axis from the surface toward the substrate and also in the surface plane. The probed region can be estimated to be the order of the area of the laser spot, i.e., a circle $\sim$100 μm of diameter and with a depth corresponding to the laser beam penetration (which is $\sim$0.5 μm for He–Ne laser line) enlarged by the carrier diffusion, resulting in approximately a few microns in depth. We observed that the strain gradient in the plane of the film around a radius of 0.5 mm at the ring center is small (corresponding to the broadening smaller than 1 meV). In this case, the major contribution is due to the strain gradient along the z axis. The estimated broadening from this effect using Eqs. (7) and (9) is in good agreement with the experimental data ($\Delta\epsilon/\epsilon\sim5\%$ for $\epsilon=0.22\%$).

B. Magneto-excitons in InP

We performed magneto-PL experiments in the InP sample at 2 K under biaxial tensile strain. A magnetic field of up to 15 T was applied parallel to the growth axis. The behavior of the PL spectra of the InP sample with the strain is very similar to that shown for the GaAs sample. Figure 3

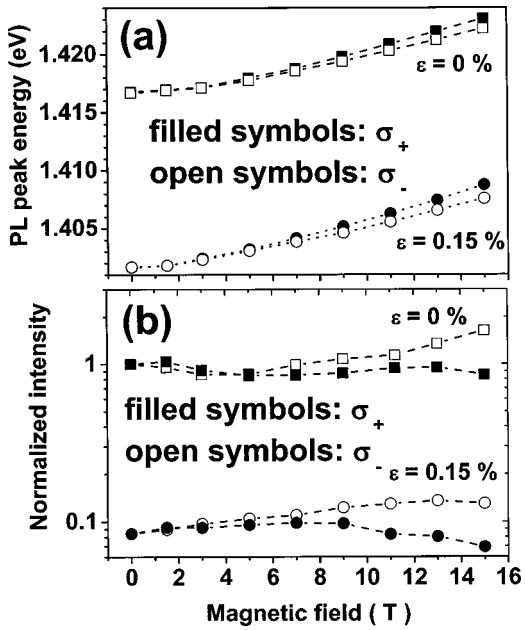

FIG. 4. PL peak energies (a) and their normalized intensities (b) as a function of the magnetic field. σ_+ and σ_- indicate right and left circular polarization of the emission light.

shows typical PL spectra of the InP sample for the unstrained case ($\epsilon=0$), where the PL emission consists of bound bulk excitons associated with a shallow impurity, and when the sample is strained ($\epsilon=0.15\%$), where the optical emission is only due to the LH bound exciton. The PL spectra show an additional peak which is not resolved for $\epsilon=0$ and resolved for $\epsilon=0.15\%$. It is related to a bound exciton associated with a different shallow impurity. Under a magnetic field, the PL peak suffers a blueshift due to the diamagnetic effect. The Zeeman effect is clear in our PL spectra. The splitting of the spin degeneracy of the exciton peaks is obtained by selecting the appropriate circularly polarized signal, resolving the two optical active exciton components: σ^+ corresponding to angular momentum $m=+1$ and σ^- for $m=-1$.

The PL peak energy and their intensity as a function of the magnetic field are presented in Fig. 4. The PL peak energies for both unstrained and strained cases shift to higher energies when the magnetic field increases and show a clear Zeeman splitting [Fig. 4(a)]. Their intensities are also dependent on the magnetic field. The intensity of the σ^+ component diminishes, while σ^- increases for increasing magnetic field, as shown in Fig. 4(b). This result shows the thermal occupation of the splitting levels. The PL peak shift is dominated by the diamagnetic effect, which is presented in the two field regimes in Fig. 5: a quadratic behavior for lower magnetic fields ($B<7$ T) and a linear one for higher ones. The diamagnetic shift is more pronounced when the sample is strained. For $\epsilon=0\%$ the variation in PL peak shift is 40 μeV/T^2 and 496 μeV/T in the quadratic and the linear regimes, respectively, while for $\epsilon=0.15\%$ they are 52 μeV/T^2 and 522 μeV/T. This behavior can be qualitatively explained in terms of the reduced effective mass of the excitons. For the unstrained case the average reduced effective mass due to the LH and HH excitons is $\mu_{us}=0.0565m_e$, while for strained case (which corresponds to the LH exciton only) is

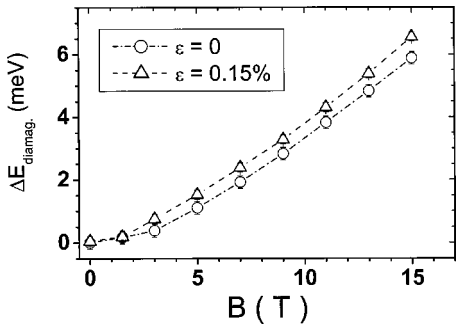

FIG. 5. Diamagnetic shift as a function of the magnetic field obtained from the data of Fig. 4(a) for $\epsilon=0$ and 0.15%.

$\mu_s=0.047m_e$. Since the diamagnetic shift is inversely proportional to the effective mass[16] under the low field regime, it must be higher for the strained system, which is in qualitative agreement with the results of Fig. 5. Quantitatively, the value of the ratio $\mu_{us}/\mu_s\sim1.2$ is also consistent with the ratio of the coefficients of the quadratic terms given above (52/40=1.3), since the average size of the wave function of the excitons is very similar to both cases.

In Fig. 6 we present the Zeeman splitting energy as a function of the square of the magnetic field for both the unstrained and strained ($\epsilon=0.15\%$) cases. We expected that the Zeeman splitting presents a quadratic behavior within our experimental field range due to the anisotropy of the valence bands.[17–19] Fitting the experimental data in Fig. 6 with a splitting energy of the form $\Delta E=aB^2$, we obtained $a=4.1\pm0.2\,\mu\mathrm{eV\,T^{-2}}$ for the unstrained case and $a=5.4\pm0.1\,\mu\mathrm{eV\,T^{-2}}$ for a strain of 0.15%. We note that the Zeeman splitting energies slightly increase for the sample under biaxial tensile strain. This behavior is opposite to what one would expect, since in the strained case the PL is due to the LH emission only and the effective Landé g factor for this exciton should be smaller than that for the HH exciton.[20] However, the complex nature of the valence bands might lead to band mixing effects, with a corresponding influence on the g factor. We therefore conclude that such contribution cannot be estimated without more realistic calculations. The investigation of the origin of this increase on the Zeeman

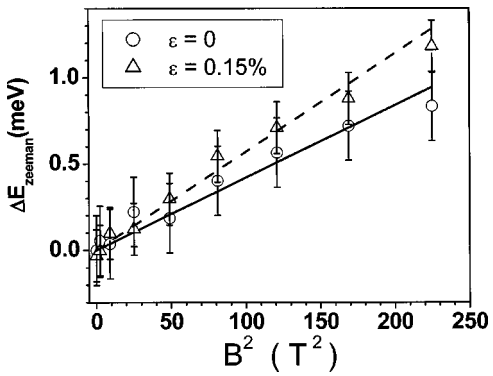

FIG. 6. Zeeman splitting energies as a function of the square of the magnetic field for $\epsilon=0$ and 0.15%. The dashed and continuous straight lines are fitting curves of the quadratic dependence of the Zeeman splitting energies with the magnetic field.

splitting energy with the tensile biaxial strain is still in progress.

ACKNOWLEDGMENTS

The authors thank Milton M. Tanabe and André R. de Paula for technical assistance in building the stress ring system and acknowledge financial support from FAPESP, CAPES, CNPq, and FINEP.

[1] J. M. Smith, P. C. Klipstin, R. Grey, and G. Hill, Phys. Rev. B **57**, 1746 (1998).
[2] J. M. Mercy, C. Bousquet, J. L. Robert, A. Raymond, G. Gregoris, J. Beerens, J. C. Portal, and P. M. Frijlink, Surf. Sci. **142**, 298 (1984).
[3] G. Gregoris, J. Beerens, S. Ben Amor, L. Dmowski, J. C. Portal, D. L. Sivco, and A. Y. Cho, J. Phys. C **20**, 425 (1987).
[4] O. P. Hansen, J. S. Olsen, W. Kraak, B. Saffian, N. Ya. Minina, and A. M. Savin, Phys. Rev. B **54**, 1533 (1996).
[5] K. I. Kolokolov, A. M. Savin, S. D. Beneslavski, N. Ya. Minima, and O. P. Hansen, Phys. Rev. B **59**, 7537 (1999).
[6] H. A. P. Tudury, M. K. K. Nakaema, F. Iikawa, J. A. Brum, E. Ribeiro, W. Carvalho, Jr., A. A. Bernussi, and A. L. Gobbi, Phys. Rev. B **64**, 153301 (2001).
[7] M. L. W. Thewalt, D. A. Harrison, C. F. Reinhart, and J. A. Wolk, Phys. Rev. Lett. **79**, 269 (1997).
[8] G. H. Loeckel, N. G. Cave, and J. Menéndez, Appl. Phys. Lett. **66**, 3639 (1995).
[9] M. Z. Maialle, Phys. Rev. B **61**, 10877 (2000).
[10] V. V. Baptizmanskii, I. I. Novak, and Y. F. Titovets, Sov. Phys. Solid State **21**, 1915 (1979).
[11] E. Liarokapis and W. Richter, Meas. Sci. Technol. **3**, 347 (1992).
[12] M. Filonenko-Borodich, in *Theory of Elasticity* (Peace, Moscow, 1966).
[13] F. Iikawa, F. Cerdeira, C. Vazquez-Lopes, P. Motisuke, M. A. Sacilotti, R. A. Masut, and A. P. Roth, Phys. Rev. B **38**, 8473 (1988).
[14] Landoldt-Börnstein, in *Numerical Data and Functional Relationship in Science and Tecnology*, edited by O. Madelung (Springer, Berlin, 1982), Vol. III/17a.
[15] G. Bastard, in *Wave Mechanics Applied to Semiconductor Heterostructures* (Les Editions de Physique, Paris, 1992).
[16] C. Cohen-Tannoudji, B. Diu, and F. Laloë, in *Quantum Mechanics* (Wiley, New York, 1977), Vol. 1.
[17] W. Edkart, K. Losch, and D. Bimberg, Phys. Rev. B **20**, 3303 (1979).
[18] D. Bimberg, K. Hess, N. O. Lipari, J. U. Fischback, and M. Altarelli, Physica B & C **89**, 139 (1977).
[19] J. I. Pankove, in *Optical Process in Semiconductors* (Dover, New York, 1975).
[20] Y. Chen, B. Gil, H. Mathieu, and J. P. Lascaray, Phys. Rev. B **36**, 1510 (1987).